Available online at www.sciencedirect.com

ScienceDirect

Energy Procedia 49 (2014) 1652 – 1663

Energy Procedia

SolarPACES 2013

Influence of different operation strategies on transient solar thermal power plant simulation models with molten salt as heat transfer fluid

P.H. Wagner[a], M. Wittmann[a]*

[a]*Institute of Solar Research, DLR German Aerospace Center, Institute of Solar Research, Pfaffenwaldring 38-40, 70569 Stuttgart, Germany*

Abstract

One of the advantages of solar thermal power plants (STPPs) with molten salt as heat transfer fluid is the direct storage system. This means that the thermal energy collected by the solar field and the electric power generation can be fully decoupled. The plant operator must therefore make the daily decision when to start-up or to shut-down the power block (PB). Normally, the solar field of these STPPs is overdesigned which leads to dumping of solar energy during days with high solar radiation, due to the inability of the hot tank and the PB to consume all the collected thermal energy. The PB must therefore start as soon as possible to prevent excessive dumping of solar energy. Contrarily, on days with low solar radiation, the PB should not start too early to prevent a second start-up on this day, because of a low hot tank level. In order to operate within these counter bounds, a fixed and a dynamic operation strategy are proposed. The so-called solar-driven strategy serves as a reference. Using this strategy, the PB operates whenever the solar field is online. The two proposed operation strategies are compared to the reference strategy by means of a transient STPP simulation model. Using the dynamic operation strategy, the annual unnecessary PB start-ups and the auxiliary heater thermal energy for anti-freeze protection are decreased, whereas the annual net electricity is increased.

Selection and peer review by the scientific conference committee of SolarPACES 2013 under responsibility of PSE AG.
Final manuscript published as received without editorial corrections.

Keywords: operation strategy; molten salt; solar thermal power plant; parabolic trough collector; concentrated solar power; dynamic modeling; start-up; shut-down sequences; guiSmo

1. Introduction

Most solar thermal power plants (STPPs) that are currently being run, harvest solar energy by parabolic trough collectors (PTCs). The energy is then transferred via synthetic oil to the thermodynamic steam cycle. The use of

* Corresponding author. Tel.: +49-711-6862-730; fax: +49-711-6862-8032.
E-mail address: michael.wittmann@dlr.de

Selection and peer review by the scientific conference committee of SolarPACES 2013 under responsibility of PSE AG.
Final manuscript published as received without editorial corrections.
doi:10.1016/j.egypro.2014.03.174

Nomenclature

DNI	Direct normal irradiance (W/m²)
j	Control variable from 0 to n (-)
E	Energy (J)
ṁ	Mass flow (kg/s)
Q	Specific energy (J/m²)
Q̇	Power (W)
r	Ramp up factor (kg/s/s)
t	Time (s)
z	Hot tank level (-)

Greek letters

η	efficiency (-)

Subscripts

D	at the design point
dyn	dynamic
e	electrical
fix	fixed
hl	heat losses
th	thermal

Abbreviations

AH	Auxiliary heater
BOP	Balance of plant
CF	Cold feeder
CH	Cold header
HF	Hot feeder
HH	Hot header
HT	Hot tank
HTF	Heat transfer fluid
IS	Indirect storage
LCoE	Levelized cost of electricity
MM	Mass multiplier
OPS	Operation strategy
PB	Power block
PF	Profile
PTC	Parabolic trough collector
PTR	Parabolic trough receiver
SF	Solar field
SEGS	Solar Energy Generating System
STPP	Solar thermal power plant

oil as heat transfer media has some drawbacks. The limitation to higher process temperature is regarded as the major drawback for efficiency improvements and, thus, lower electricity costs.

Molten salts as an alternative heat transfer fluid (HTF) for parabolic trough systems show a potential for lowering the levelized cost of electricity (LCoE). Kearney et al. [1] described a possible reduction of LCoE between 14.2 to 17.6% depending on the salt mixture. Turchi et al. [2] approved the LCoE reduction potential, as he published reductions of 6 to 15% depending on different solar field (SF) sizes. Kelly et al. [3] showed that for the case of changing the HTF to salt and the PTC to a more suitable 8-meter aperture, LCoE reduction of 25% are realistic. Kolb and Diver [4] approved this figure. In Wittmann et al. [5] the influence on storage size, high and low process temperature, and employed salt have been assessed. It was demonstrated that further optimization potential can lead to further LCoE reductions.

In STPP energy yield calculation an operation strategy (OPS) which represents the power plant operator has to be defined. Most of the calculations are conducted by using the so-called solar-driven OPS, as described in Eck et al. [6]. It means that the operator's goal is to synchronize the plant to the grid whenever the current solar irradiation situation and the thermal storage charge allow the operation. In reality, the operator does not only use the current state as basis for any operational decision, but also the weather forecast. By looking to the future, the operator is able to reduce non-reasonable power block (PB) starts and stops, and therefore enhance the electricity output.

Lippke [7], and Cerni and Price [8] were the first to publish research on the impact of operational strategies on the SEGS power plant's electricity output. Lippke evaluated the optimal operational SF temperature under different operating conditions. Cerni and Price [8] introduced weather forecasts in order to set up the daily operation schedule. They intended to increase the annual energy generation through more prudent use of the limited natural gas allotment, and through improved maintenance planning. Wittmann et al. [9,10] used mathematical optimization in order to raise the revenues of commercial STPPs under uncertainty of weather and price forecasts. Powell et al. [11] also based their optimizations on weather forecasts. Regarding the classification according to Hirsch et al. [12] the mentioned three works are classified in the high quality level models. García-Barbarena et al. [13] showed the influence on gas consumption of the auxiliary heater (AH). All authors mentioned in this paragraph assessed STPPs

based on thermal oil as HTF and PTCs. Only Powell [11] uses a HTF which serves as well as storage media. All authors use storage systems except Gariá-Barbarena et al. [13].

In this paper the fixed and dynamic OPS are proposed which are compared to the typically used solar-driven OPS. The fixed OPS is classified to medium, and the dynamic OPS to high quality level acc. to Hirsch et al. [12]. In order to run the thermodynamic assessment of the three OPS, a transient model that represents a fully integrated STPP is set up and explained. This STPP with molten salt as heat transfer medium is equipped with a huge thermal energy storage system, and located at a highly sunny site in Las Vegas, Nevada.

2. Technical model setup

The transient STPP simulation model [14] is created with the commercial simulation software EBSILON®Professional, referred to as Ebsilon in this paper, by Steag Energy Services GmbH. Hereby the add-ons EbsSolar [15] and EbsScript are used to model the SF and the OPS, respectively. The Ebsilon time series dialogue is used to perform annual yield calculations like described in Hirsch et al. [16]. The following section gives the SF and PB simulation model, and their transient system behavior. It introduces a reference plant and its parameters, whereby the three different OPS can be compared.

2.1. Solar field

The model of the SF consists of the sun, parabolic trough collectors, distributing and collecting headers, feeders, two salt submersion pumps, an auxiliary heater, and a cold and hot storage tank. Fig. 1 (c) contains a schematic drawing of the Ebsilon simulation model.

If solar radiation is available, the molten salt from the cold tank is pumped through the collectors. It is heated up to the design temperature of 530 °C and stored in the hot tank (HT). If the HT is filled to its minimum charging level for production, the production process can begin upon demand for electricity: The molten salt is pumped through the steam generator in the PB, exchanges its heat with the water steam circuit, and returns to the cold tank.

In the Ebsilon model, the SF or the HT can be maintained with HTF at 530 °C by activating the model of the AH and pumping the HTF through the corresponding loops, the A) HT or B) SF support loop, shown in Fig. 1 (c). During nighttime operations, the HTF from the SF is pumped through the C) recirculation loop to the cold tank. This recirculation of the HTF is necessary to prevent solidification. If the cold tank reaches its critical temperature during nighttime cool-down (305 °C), HTF from the HT is pumped through the D) cold tank support loop to prevent the HTF in the SF from reaching its critical temperature.

The solar heat input into the HTF is simulated with components C1, C2, C3, and C4, representing a PTC loop. This heat input depends on the boundary conditions of normal solar irradiation, the location, and the current date and time. End losses, shading losses, an average cleanliness factor (0.98), and availibility(0.98) are considered. In order to model transient start-up and shut-down processes, each collector is connected in serial with an indirect storage (IS) element which simulates the PTC thermal inertia. Therefore, the component C1 and IS1 form the transient PTC1, the component C2 and IS2 form the transient PTC2, and so on [17]. The interconnectors between two PTCs are modeled with the piping element P2. The mass flow through the PTCs is controlled so that the HTF reaches the HT design temperature at the SF outlet.

As shown in Fig. 1 (a) several PTC loops are connected by the distributing / cold (blue line) and collecting / hot header (red line) and form one sub-field, whereas several sub-fields are connected by hot and cold feeders with the balance of plant (BOP). These sub-fields are arranged within the 3/2 H layout which is proposed for the next-generation STPP up to 250 MW_e [18].

All individual layout components, labeled in Fig. 1 (a), are represented by certain Ebsilon simulation components, given in Fig. 1 (c). The simulation models only one representative PTC loop for the layout, marked with a red dashed ellipse in Fig. 1 (a), which simulates the pressure drop, thermal loss and the thermal inertia of all other PTC loops in the SF. The cold feeder (CF) and cold header (CH), which are colored blue in Fig. 1 (a), are represented by the components P1, and H1, respectively. No indirect storage components are added, because the temperature change over time in the cold piping elements is far less than that in the hot piping elements. Considering the hot piping site, the HTF and piping elements temperature nears solidification temperature during nighttime and

upper HTF temperature during normal daytime SF operation. This piping site, which is colored red in Fig. 1 (a), is therefore modeled transient. The hot header (HH) and hot feeder (HF) are represented by the components H2 and IS5, and P3 and IS6, respectively. To approximate the 3/2 H layout, the Ebsilon simulation uses a simple model. Mass multipliers (MM) are introduced into the simulation model in order to simulate the representative loop. They divide or multiply the HTF mass flow in the pipe with a specific factor.

Heat losses of the hot and cold tank, piping elements (components P1 to P3), and parabolic trough receivers (component C1 to C4) realistically model the HTF's nighttime cool-down behavior. The 2008 Schott PTR 70 model, tested at NREL, is used [19]. The piping elements heat loss is modeled by means of a linear equation using the heat loss factor for pipes assumed to 200 W/m². Experiences from the Andasol project [20] are used to estimate the tank heat loss of any other size, or upper and lower tank temperature, by assuming a constant specific heat flow through the tank walls [14]. The pressure losses in the parabolic trough receiver (PTR) and the piping components are used to simulate the parasitics of the two submersion pumps (SP1 and SP2). This allows an estimation of the pump electricity consumption for the annual yield calculation. The SF thermal inertia is approximated by entering the steel and HTF mass of all PTRs, collecting headers, and feeders (components IS1 to IS6) into the simulation model. The real cascaded header's thermal inertia is approximated by a simple pipe with constant inner diameter (component IS5), the representative header, like described by Hirsch and Schenk [21]. Additionally, the steel mass of the representative header is chosen in order that it is equal to the steel mass of the real cascaded header [14].

As stated, the transient system behavior of the SF is modeled by the indirect storage component. It is a simple pipe model that simulates transient heat exchanges between the pipe and the fluid flowing through. The two-dimensional Fourier differential equation, rotational symmetry of the pipe is assumed, is discretized using the finite volume method on an approximately 30x30 Cartesian grid, which represents the wall of the indirect storage component. The time is discretized using the Crank-Nicolson method [22]. Transient processes are simulated within a time step of 10 seconds. The size of a local volume cell is chosen in order that the Courant number is less than 1.

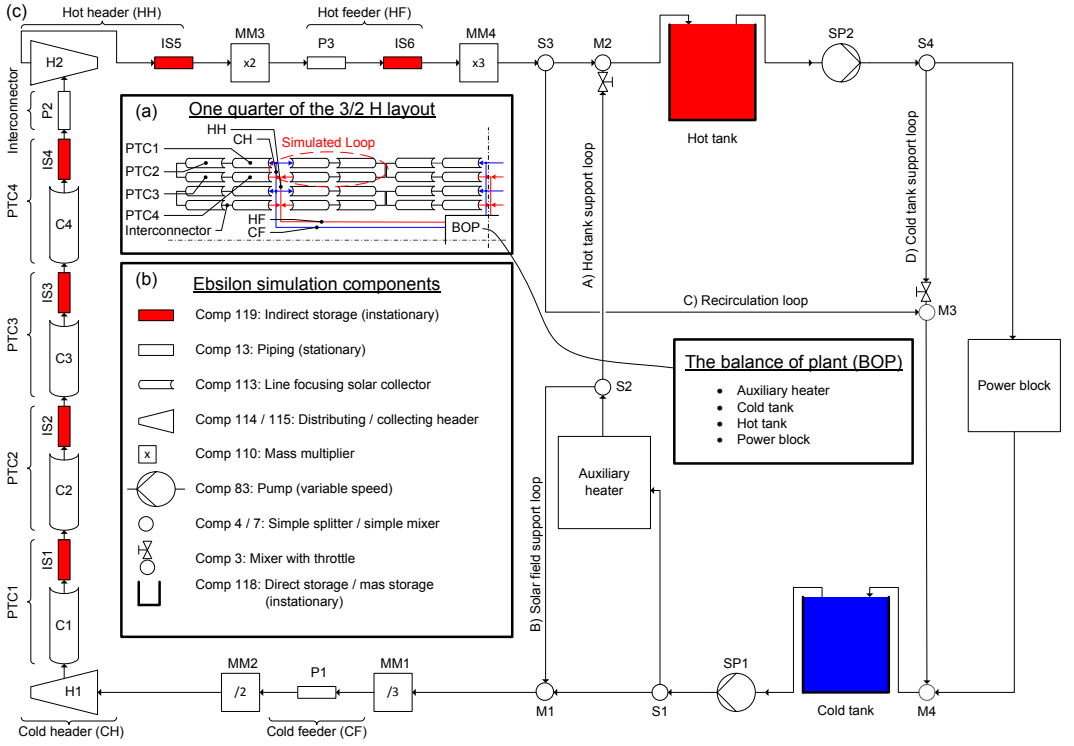

Fig. 1. (a) Schematic of one quarter of the 3/2 H layout with all individual components which are represented by certain (b) Ebsilon simulation components in the (c) solar thermal power plant simulation model.

2.2. Power block

The PB is based on a conventional thermal power plant with re-heat and steam extraction from six turbine stages [14]. It consists of a steam generator, steam turbine, generator, condenser, and feed water heating. The sub-critical steam generator, a once-through boiler, is the only non-conventional part. It is modeled as a Benson once-through type. The water is preheated, evaporated, and superheated in one single pass. During off-design conditions, the start and end point, as well as the length of the evaporation zone, shifts inside the tubes according to the mass flow of the HTF and feed water. Water recirculation and injection for very low steam generator off-design behavior is not implemented.

The transient behavior of the PB is not modeled as much detail, as that of the SF. Instead of modeling full transient behavior, the model assumes a pseudo-transient one. A PB energy state ($\Delta E_{PB,th}$) is therefore introduced that models the current energy stored in the PB

$$\Delta E_{PB,th} = \int_{t_0}^{t} \dot{Q}_{PB,th}(t)\,dt \approx \sum_{j=1}^{n} \dot{Q}_{PB,th,j}\Delta t \tag{1}$$

using the thermal energy flow into the PB ($\dot{Q}_{PB,th,j}$) at a specific time instant (j) with the time series time step of 10 minutes (Δt=10 min). The required start-up PB energy is assumed by a simple ansatz.

$$E_{PB,th,start-up} = \frac{\dot{Q}_{PB,e,D}}{\eta_{net,D}} \Delta t_{start-up} \tag{2}$$

The start-up time ($\Delta t_{start-up}$) is introduced to estimate the thermal power needed for the PB startup. This time is multiplied by the thermal input to the PB at the design point ($\dot{Q}_{PB,e,D}/\eta_{net,D}$) and is assumed to half an hour. The duration of the startup increases with PB downtime. Because the literature provides no cool-down data for a PB with a once-through boiler and salt as HTF, the model assumes that PB heat losses during standby operations ($\dot{Q}_{PB,hl,stand-by}$) are 1% of PB thermal energy input during operations at the design point ($\dot{Q}_{PB,th,D}$).

$$\dot{Q}_{PB,hl,stand-by} \approx 0.01 \cdot \dot{Q}_{PB,th,D} \tag{3}$$

During PB standby mode, a salt mass flow whose thermal power corresponds to $\dot{Q}_{PB,hl,stand-by}$ passes through the steam generator to maintain hot temperatures, and as a result, the start-up time ($\Delta t_{start-up}$) is assumed to be constant. The PB state is assumed online when current energy stored in the PB in Eq. 1 is equal to required start-up PB energy in Eq. 2 ($\Delta E_{PB,th}=E_{PB,th,start-up}$).

Besides the PB thermal inertia, the start-up process is also delayed due the mass inertia of the steam turbine. High temperature gradients are also to be avoided to reduce thermal strain, so the speed of the heating process is limited. To account for these factors, the simulation introduces the ramp-up factor (r) with the unit kg/s/s. This factor allows the mass flow into the PB at a given time

$$\dot{m}_{PB}(t) = \dot{m}_{PB,30\%-load} + r(t - t_0) \tag{4}$$

to be calculated using the mass flow into the steam generator at 30% PB load ($\dot{m}_{PB,30\%-load}$) and the beginning time of the startup (t_0). The factor r is assumed to 100 kg/s/600s.

2.3. Model inputs

Las Vegas has been chosen as the reference plant location. The DNI and temperature inputs into the simulation are made from the 2008 Las Vegas solar data set provided by NREL [23]. A ten-minute resolution of data input is chosen in order to correctly simulate the transient plant processes [14]. Most model inputs are adapted from results of the HPS project [24] in order to obtain an appropriate setup.

Table 1 lists the plant site, solar field, parabolic trough collectors, storage system, AH, and the PB parameters. The SF's layout is the 3/2 H layout, which consists of 372 collector loops, each consisting of four Eurotrough ET150 collectors with PTR 70 receiver. The STPP solar multiple, the ratio of thermal power from the SF at the design point to thermal power into the PB at 100% load, is assumed to be 2.4. Each storage tank has a capacity of 35,349 metric tons of solar salt and is able to feed the steam generator for 12 hours to produce electricity. The design temperature is assumed to be 530 °C for the HT and 305 °C for the cold tank. During transient start-up or shut-down, the molten salt from the SF is pumped to the HT if its temperature is higher than 485 °C, and to the cold tank if its temperature is lower. The lowest temperature of the heat transfer fluid (solar salt) during night operations is assumed to be 270 °C in order to ensure a safety clearance above the molten salt's liquidus temperature of 240 °C. The nominal AH power output is 84 MW_{th} what corresponds to 30% of the PB thermal input at the design point. The overall PTR and piping steel mass is 1,778 t and the HTF mass in the pipes is 2,590 t.

The PB's gross capacity is 125 MW_e, the live steam parameters are 520 °C and 150 bar, and the reheated steam parameters are 520 °C and 30 bar. The parameters for the pseudo-transient behavior of the PB are assumed to be 0.5 h for the start-up time ($\Delta t_{start\text{-}up}$) in Eq. 2, and 100 kg/s/600s for the ramp-up factor (r) in Eq. 4.

Table 1. The reference plant parameters.

Plant site: Las Vegas, Nevada (GMT -8)			
Latitude, longitude,	36.06° N, 115.08° W	Annual direct normal irradiation (kWh/m²/y)	2659
Solar field			
Solar multiple (-)	2.4	Gross aperture area (km²)	1.27
Layout	3/2 H	Heat transfer fluid	Solar salt
Collectors per loop	4	Lowest HTF temperature (°C)	270
Loops per sub-fields	62	Total HTF mass in all hot feeders and headers (t)	1,310
Sub-fields	6	Thickness of pipes (mm)	71
Area (km²)	2.14 (W to E) x 2.00 (N to S)	Total hot feeders and headers steel mass (t)	662
Parabolic trough collectors			
Typ	Euro-Trough 150	Absorber tube outer diameter (m)	0.07
Receiver	Schott PTR 70	Absorber tube inner diameter (m)	0.064
Peak optical efficiency (%)	76.8	Total receiver steel mass (t)	1,116
Mirror cleanliness factor (%)	98	Total HTF mass in all receivers (t)	1,281
Storage System			
Hot tank design temperature (°C)	530	Storage time (h)	12
Cold tank design temperature (°C)	305	HTF mass in each storage tank (t)	35,349
Auxiliary heater			
Nominal capacity (MWh_{th})	84	Efficiency (%)	90
Power block at design point			
Gross capacity (MW_{el})	125	Turbine back-pressure (bar)	0.08
Live steam temperature (°C)	520	Gross efficiency (%)	44.69
Live steam pressure (bar)	150	Net efficiency (%)	44.30
Reheated steam temperature (°C)	520	Ramp-up factor (kg/s/s)	0.1667
Reheated steam pressure (bar)	30	Start-up time (h)	0.5

Table 2. The eight solar thermal power plant operation mode possibilities referred to as profiles (PFs) 1 to 8.

Stationary solar field state					Transient solar field state				
PF	SF	AH	PB	Description	PF	SF	AH	PB	Description
1	X	0	X	Stationary SF and PB operation, AH is off	6	X	0	X	Transient SF operation, stationary PB operation, AH is off
2	X	0	0	Stationary SF operation, PB is on standby, AH is off	7	X	0	0	Transient SF operation, PB is on standby, AH is off
3	0	0	X	SF is on standby, stationary PB operation, AH is off	8	X	X	0	Transient SF operation, PB is on standby, AH supports HT
4	0	0	0	SF and PB are on standby, AH is off					
5	0	X	0	SF and PB are on standby, AH supports HT					

3. Assessment of operation strategies

The simulation model consists of three separate units: the solar field, the auxiliary heater, and the power block. Because of the SF's ability to operate in stationary or transient mode, twelve different STPP operation modes are possible. The simulation model uses eight of them, listed in Table 2.

Before the model simulates a given time instant, it selects one of the eight profiles. Each profile imports various process parameters into the simulation model. The first step is determining whether the SF simulation mode is stationary or transient. A transient simulation starts at sunrise and lasts until the HTF temperature reaches the HT design temperature (530 °C), or until it is below the lowest HTF temperature during nighttime circulation (270 °C) and the sun has set. This occurs when there is not enough solar radiation to start-up the SF during daytime. Transient processes during daytime, e.g. clouding or end-of-day shut-down, last until the HTF reaches the HT design temperature or the lowest HTF nighttime circulation temperature. During daytime, the SF can operate stationary or transient if a minimum predicted salt mass flow from the SF is secured. Otherwise the SF is on standby, what means HTF from the cold tank is recirculated over the SF. The AH always operates if the HT reaches a threshold level (z_{AH}=0.003), as shown in Fig. 2 (a). The PB is able to operate if the HT minimum level is reached. The model offers three different basic OPS:

- Solar-driven operation strategy (reference OPS)
- Fixed operation strategy (FIX OPS)
- Dynamic operation strategy (DYN OPS)

In the reference OPS, the PB starts whenever the HT level rises to the PB shut-down threshold (z_{PB} = 0.03), whereas in the FIX OPS, shown in Fig. 2 (a) on the left side, the PB starts when the HT reaches a threshold level ($z_{PB,fix}$) which can be specified in the simulation model. A high fixed PB start-up threshold causes a late PB start-up and therefore the HT reaches the maximum level earlier on days with high solar radiation. Because of this the PTCs are defocused earlier and more solar energy is dumped. A low fixed PB start-up threshold causes an early PB startup and therefore the HT reaches PB shut-down threshold (z_{PB}) earlier on days with low solar radiation. Because of this, the PB shuts down and eventually has to start-up a second time, if the HT reaches the fixed PB start-up threshold again during that day. On such a day the PB consumes more thermal energy for the heat-up during the start-up process. Another disadvantage is that the PB is in off-design modus for a longer time and the overall PB efficiency is therefore lower.

To tackle these problems, the model can use the DYN OPS which is shown in Fig. 2 (a) on the right site. For each day of the simulation, the PB start-up threshold changes dynamically between a minimal ($z_{PB,dyn,min}$) and a maximal threshold ($z_{PB,dyn,max}$) according to the daily weather conditions (24 hour forecast). The dynamic PB start-up threshold is therefore a function of the DNI ($z_{PB,dyn}$=f(DNI)). Like in the FIX OPS the PB operates until the HT reaches the PB shut-down threshold (z_{PB}). To identify the day-to-day dynamic PB start-up threshold, the model uses two decision criteria. First one is the day's maximum DNI.

$$\mathrm{DNI}_{\max} = \max\left(\mathrm{DNI}(t)\right) \tag{5}$$

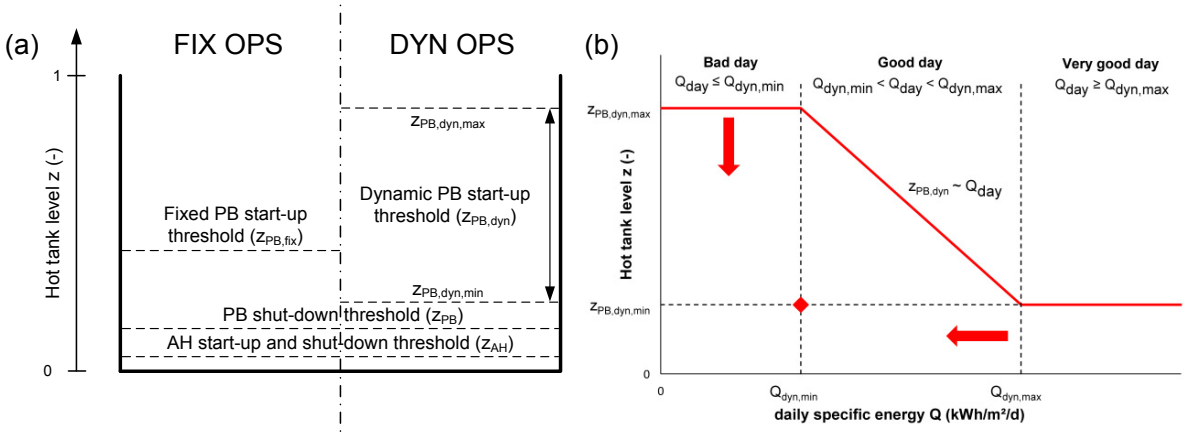

Fig. 2. (a) Comparison of the HT threshold levels for the FIX OPS (left side) and the DYN OPS (righ side); (b) The three different types of days that can occur in the DYN OPS, their conditions, and the PB start-up thresholds.

The second is the collected solar energy over one specific day

$$Q_{day} = \int_{t_{sunrise}}^{t_{sunset}} DNI(t)\,dt \approx \sum_{j=1}^{\frac{t_{sunset}-t_{sunrise}}{\Delta t}} DNI_j \Delta t \tag{6}$$

which is approximated by the sum of DNI at one specific time series time step (DNI_j) and the time series time step (Δt). This energy is compared to the DYN OPS maximum ($Q_{dyn,max}$) and minimum ($Q_{dyn,min}$) specific day energy. Therefore three different situations can occur which refer to three different types of days (bad, good, and very good day) that are shown in Fig. 2 (b). A bad day refers to a day where the solar energy is lower than the DYN OPS minimum specific day energy ($Q_{day} \le Q_{dyn,min}$), whereas it is higher than the DYN OPS maximum specific day energy ($Q_{day} \ge Q_{dyn,max}$) for the very good day, respectively. The dynamic PB start-up threshold on good days ($Q_{dyn,min} < Q_{day} < Q_{dyn,max}$) is approximated by a linear function. The PB does not operate at all if the day's maximum DNI is lower than the minimum PB start-up DNI ($DNI_{max} \le DNI_{PB,min}$) which refers to a cloudy or very bad day.

To find appropriate OPS parameters for the presented STPP in Las Vegas during the year 2008, a variation of the parameters $Q_{dyn,max}$ and $z_{PB,dyn,max}$, as shown by the red arrows in Fig. 2 (b), is carried out. The point ($Q_{dyn,min}$,$z_{PB,dyn,min}$), marked with a red hash key in Fig. 2 (b), is fixed. All parameters for the OPSs are listed in Table 3. The minimum PB start-up threshold is selected equal to the PB shut-down threshold ($z_{PB,dyn,min}=z_{PB}$) to enable a late defocusing of the PTC during a very good day. The DYN OPS minimum specific day energy is estimated by a full HT charge during the design date 06/21/2013, and depends therefore mainly on the STPP configuration.

$$Q_{dyn,min} \le \frac{E_{HT}}{A_{SF}\,\bar{\eta}_{SF,06/21}} \tag{7}$$

Table 3. Parameters used in the simulation model for the DYN OPS for the STPP in Las Vegas during the year 2008.

Parameters to identify the weather conditions of a day				**Parameters to identify whether power block can operate**			
Parameter	$DNI_{PB,min}$	$Q_{dyn,min}$	$Q_{dyn,max}$	z_{AH}	z_{PB}	$z_{PB,dyn,min}$	$z_{PB,dyn,max}$
Value	300 W/m²	5 kWh/m²/d	8, 9, 9.5, and 10 kWh/m²/d	0.003	0.03	0.03	0.03 – 0.49

This equation uses the total gross aperture area of the PTCs (A_{SF}), the HT storage capacity (E_{HT}), and the average SF efficiency during 06/21 ($\bar{\eta}_{SF,06/21}$). In order to estimate the DYN OPS maximum specific day energy, the day when for the first or the last time of the year PTC defocusing would occur is identified

$$Q_{day} = \frac{\dot{Q}_{PB,th,D}\left(\Delta t_{day} - \Delta t_{SF,start-up} - \Delta t_{PB,start-up}\right) + E_{HT}}{A_{SF}\bar{\eta}_{SF,day}} \tag{8}$$

using the thermal energy flow in the PB at the design point ($\dot{Q}_{PB,th,D}$), the daytime of this day ($\Delta t_{day} = t_{sunset} - t_{sunrise}$), the SF start-up time ($\Delta t_{SF,start-up}$), the PB start-up time ($\Delta t_{PB,start-up}$), and the average SF efficiency of this day ($\bar{\eta}_{SF,day}$). In Fig. 3 this refers to the 18th of March with 9.72 kWh/m²/d and 24th of September with 9.01 kWh/m²/d, respectively. This situation refers to a HT full loading and PB operation during the whole daytime. The DYN OPS maximum specific day energy should therefore be less than the solar energy over this day.

$$Q_{dyn,max} \leq Q_{day} \tag{9}$$

The values 10, 9.5, 9, 8.5, and 8 kWh/m²/d for $Q_{dyn,max}$, as shown in Fig. 3, and several maximum PB start-up thresholds ($z_{PB,dyn,max}$) between 0.03 and 0.49 are compared. The calculated annual net electricity with several DYN OPSs, FIX OPSs, and the solar-driven OPS is shown in Fig. 4 a). The annual net electric output of the solar-driven OPS is 626.5 GWh_e. During the very good year 2008 in Las Vegas with 2659 kWh/m²/y, the FIX OPS cannot improve the electrical output. The negative effect of dumping solar energy due to defocusing PTCs, shown as blue line in Fig. 4 b), outweighs the positive effect of less thermal energy consumption due to less unnecessary PB start-ups, shown as blue line in Fig. 4 c). The DYN OPS with a value of $z_{PB,dyn,max}$=0.03 is equal to the solar-driven reference strategy, like it is shown by the blue line in Fig. 5. The solar-driven OPS value is therefore the limit and the other graphs converge to this value for $z_{PB,dyn,max} \rightarrow 0.03$ for all plots in Fig. 4. Comparing the DYN OPS to the solar-driven OPS, it always simulates better electric outputs of up to 631.9 GWh_e what refers to an improvement of 0.86%. The parameters 8 kWh/m²/d for $Q_{dyn,max}$ and 0.49 for $z_{PB,dyn,max}$ are identified as optimal within the investigated DYN OPS values for this STPP at the location Las Vegas during the year 2008. The DYN OPS with the value $Q_{dyn,max}$ of 10 and 9.5 kWh/m²/d is higher than the first, respectively last SF defocusing point, marked in Fig. 3. In these two strategies the annual net electricity constantly increases from a maximum PB start-up threshold

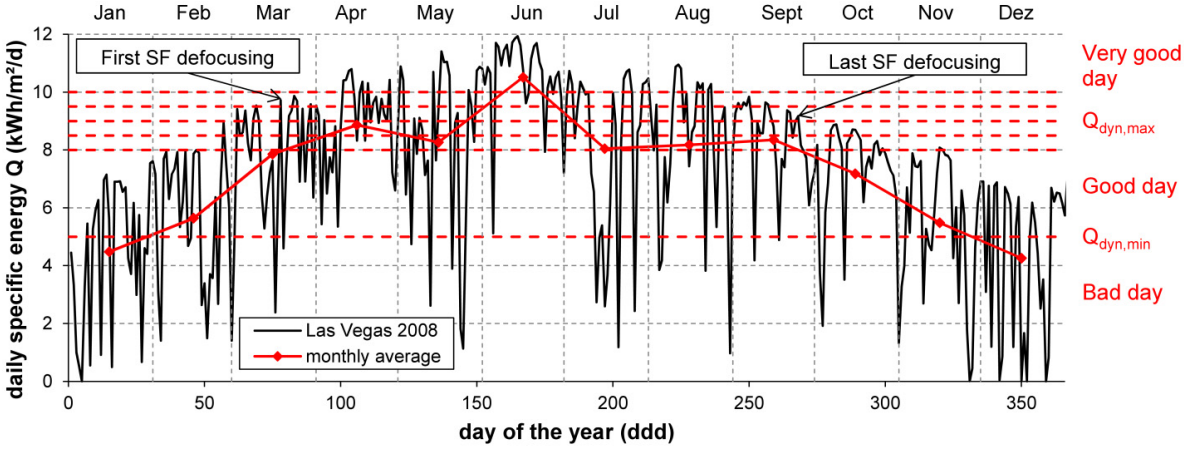

Fig. 3. The daily and monthly average specific energy in Las Vegas during 2008, the DYN OPS minimum ($Q_{dyn,min}$) and maximum specific energy ($Q_{dyn,max}$) with its five variations, and the classification of the three different days (bad, good, and very good).

of 0.49 to 0.19. The value of 0.19 for $z_{PB,dyn,max}$ is identified as the maximum for these two strategies. This refers to an aggressive strategy with early PB start-ups, also at bad days, but less SF dumping, like shown in Fig. 4 b) (red and light green lines). As stated in Eq. 9, the more reasonable values for $Q_{dyn,max}$ are 9, 8.5, and 8 kWh/m²/d. The annual net electricity maximums in Fig. 4 a) (631.35, 631.68, and 631.91 GWh_e) are at a maximum HT level of about 0.29, 0.39, and 0.49 for the DYN OPS 9, 8.5, and 8, respectively. Lower $Q_{dyn,max}$ values mean more very good days and therefore more immediately PB startups after sunrise what refers to a more aggressive OPS. Therefore the linear function slope during a good day must be higher and as a reason of this also the $z_{PB,dyn,max}$ value, like shown in Fig. 5.

The annual AH thermal energy input is kept as minimal as possible. It is assumed as constant (36 GWh_{th}) for all simulations wherefore it is possible to compare the different simulations with exactly the same energy input. The FIX and DYN OPS have a benefit, because the AH consumes less thermal energy for anti-freeze operations, and therefore the AH thermal energy can be used for electricity generation. Like shown in Fig. 4 d), the AH thermal consumption for anti-freeze decreases, respectively the AH thermal consumption for electricity generation increases, with higher PB start-up thresholds. If during a bad day the maximum HT level is not reached, the tank's thermal energy can be used during night for anti-freeze operations. Generally this happens more often for higher $z_{PB,dyn,max}$ values. Therefore DYN OPSs with high values for $Q_{dyn,max}$ and $z_{PB,dyn,max}$ consumes less gas – up to 7.72 GWh_{th}.

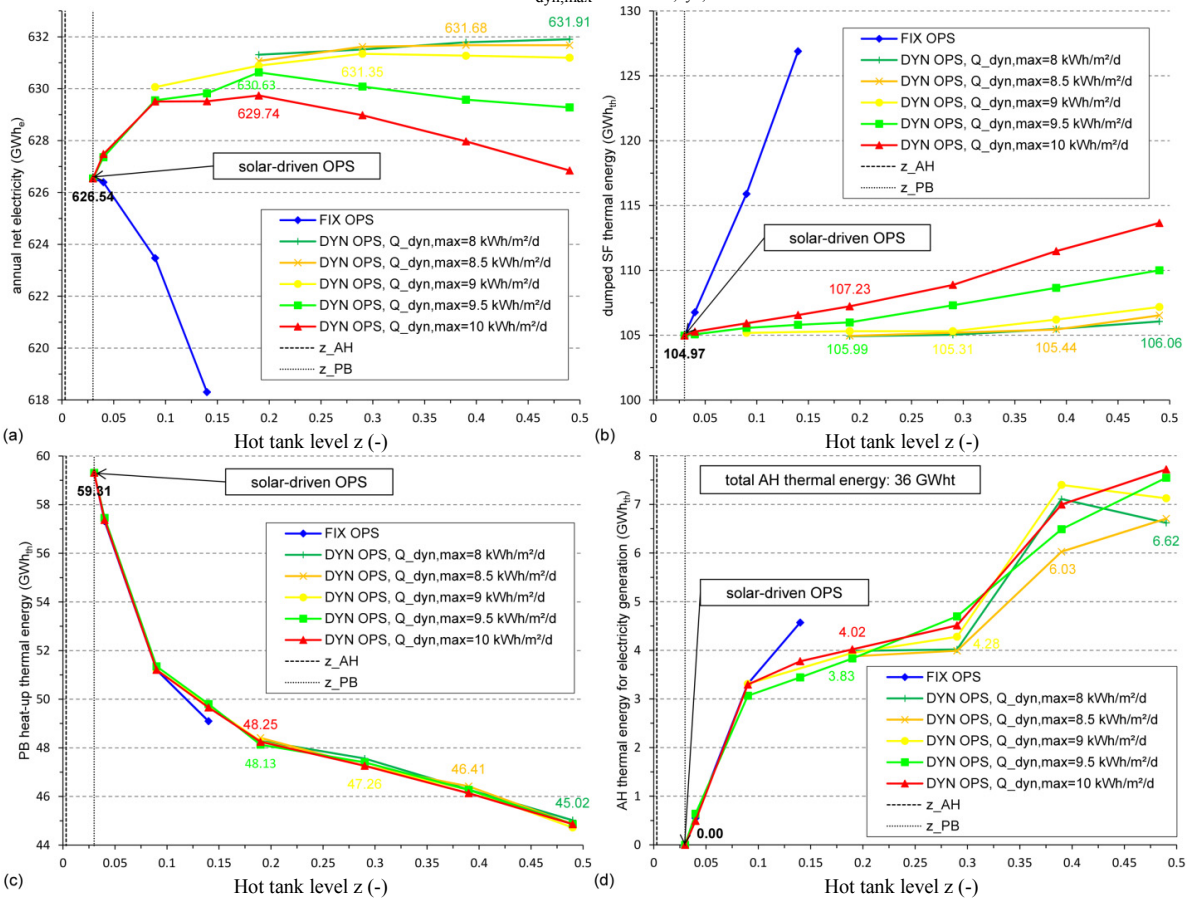

Fig. 4. Comparison of the (a) annual net electricity output, (b) dumped SF thermal energy due PTC defocusing, (c) PB heat-up thermal energy, and (d) share of the total AH thermal energy (36 GWh_{th}) for electricity generation with the solar-driven, FIX, and DYN OPS. The FIX OPS ($z_{PB,fix}$) and the DYN OPS maximum PB start-up threshold ($z_{PB,dyn,max}$) are varied, as well as the DYN OPS maximum specific day energy ($Q_{dyn,max}$) between 8 and 10 kWh/m²/d. The optimal values for the DYN OPS 8, 8.5, 9, 9.5, and 10 are marked in the corresponding colors. The values for the solar-driven reference OPS are marked black.

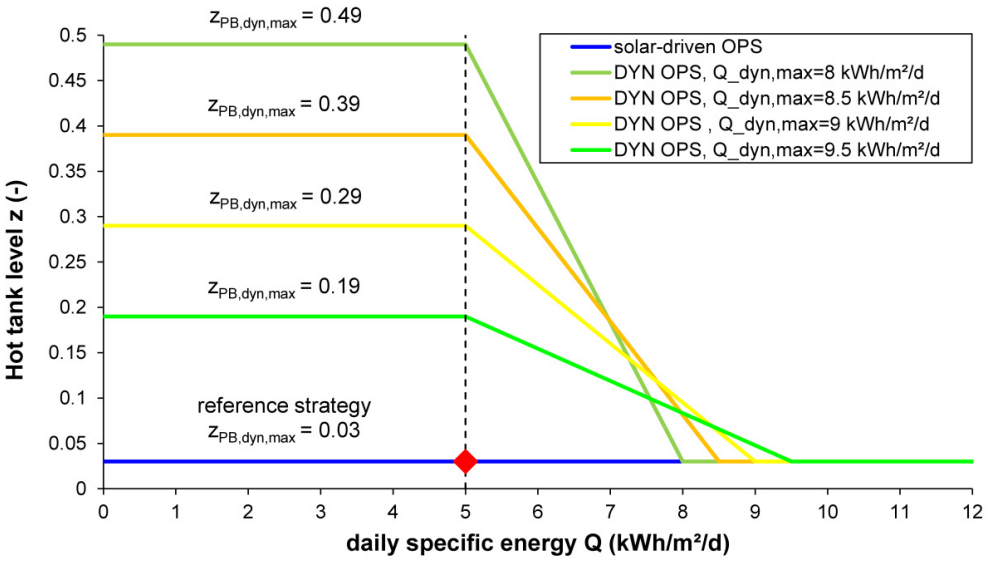

Fig. 5. The optimal DYN OPS 8, 8.5, 9, 9.5, and the solar-driven OPS which serves as reference strategy.

4. Conclusion

The proposed FIX OPS could not improve the STPP annual net electric output, because the effect of dumping solar energy due to defocusing PTCs outweighs the positive effect of less thermal energy consumption due to less unnecessary PB start-ups. Years with lower annual direct normal irradiation than the discussed 2659 kWh/m²/y, what means that more bad days and less very good days occur, should also be considered. These years need less aggressive OPS in order to avoid unnecessary PB start-ups. Because also less PTC defocusing and therefore less solar energy dumping occurs, the PB heat-up thermal energy becomes more important, and the FIX OPS could also show optimization potential. The proposed DYN OPS could show even higher optimization potential in these cases.

The DYN OPS can be easily implemented into a transient STPP simulation models, and it can simulate the operator that controls the STPP according to the daily weather forecast. In total, the DYN OPS offers six variables that can be investigated with a parametric study. Two of them, $Q_{dyn,max}$ and $z_{PB,dyn,max}$ which are considered as the most influencing, were investigated within this paper. One optimal DYN OPS for the reference STPP at the location Las Vegas during the year 2008 is presented. The results with the optimal DYN OPS parameter set show the possible potentials of the DYN OPS. The annual unnecessary PB start-ups and the auxiliary heater thermal energy for anti-freeze protection are decreased, whereas the annual gross electricity output is increased by 0.86%. Finally, these effects will also lower the LCoEs within this percentage. The exact LCoEs are not calculated in this paper.

Further optimization potential is the PB shut-down threshold (z_{PB}). It was set to 3% wherefore the thermal energy stored during the day in the HT, can be used for anti-freeze protection during nighttime. This value is set too small during winter, wherefore the AH is needed for anti-freeze protection, and too large during the summer, wherefore not all stored thermal energy is used over the night. A seasonal or daily change of z_{PB} according to the weather conditions offers therefore another optimization potential for higher annual net electric output, respectively less AH thermal energy consumption.

As mentioned, eight profiles were implemented into the STPP simulation model. Therefore four other possibilities were neglected because they require more AH thermal input and a more detailed plant OPS, e.g supporting the SF during start-up with hot HTF from the AH, producing hot HTF with the AH during nighttime and operating the PB in low off-design mode, or a combination of both. With these profiles the PB and the SF could start-up simultaneously, wherefore less dumping of solar thermal energy occurs during days with high solar radiation. Such strategies would consume more AH thermal energy and therefore more gas, but they offer also further potential for the improvement of the annual net electric output and therefore the LCoEs.

Acknowledgements

The authors would like to thank STEAG Energy Services GmbH for providing licenses of EBSILON®Professional. We also like to thank BMU for funding the HPS project, funding number #0325208. We appreciate their support very much. They also would like to thank all people who reviewed this paper and gave helpful comments.

References

[1] Kearney D, Herrmann U, Nava P, Kelly B, Mahoney R, Pacheco J, Cable R, Potrovitza N, Blake D, Price H. Assessment of a Molten Salt Heat Transfer Fluid in a Parabolic Trough Solar Field. Journal of Solar Energy Engineering 2003;125(2):170-6.
[2] Turchi C, Mehos M, Ho CJ, Kolb GJ. Current and future costs for parabolic trough and power tower systems in the US market. Proc. SolarPACES 2010, Perpignan, France; 2010.
[3] Kelly B, Price H, Brosseau D, Kearney D. Adopting nitrate/nitrite salt mixtures as the heat transport fluid in parabolic trough power plants. Proc. ASME Energy Sustainability, Long Beach, CA; 2007.
[4] Kolb G, Diver RB. Conceptual Design of an advanced Trough Utilizing a Molten Salt Working Fluid. Proc. SolarPACES 2008, Las Vegas, NV; 2008.
[5] Wittmann M, Müller-Elvers C, Schenk H, Bruce B. Optimization of Molten Salt Parabolic Trough Power Plants using different Salt Candidates. Proc. SolarPACES 2012, Marrakesh, Morocco; 2012.
[6] Eck M, Barroso H, Blanco M, Burgaleta J-I, Dersch J, Feldhoff JF, Garcia-Barberena J, Gonzalez L, Hirsch T, Ho CK, Kolb GJ, Neises T, Serrano JA, Tenz D, Wagner M, Zhu G. guiSmo: Guidelines for CSP performance modeling – Present Status of the SolarPACES Task-1 Project. Proc. SolarPACES 2011, Granada, Spain; 2011.
[7] Lippke F. The operating strategy and its impact on the performance of a 30 MWe SEGS plant. Journal of Solar Energy Engineering 1997;119(3):201–7.
[8] Cerni TA, Price H. Solar forecasting for operational support of SEGS plants. Proc. Proceedings of the 1997 American Solar Energy Society Annual Conference, Washington, DC; 1997.
[9] Wittmann M, Breitkreuz H, Schroedter-Homscheidt M, Eck M. Case Studies on the Use of Solar Irradiance Forecast for Optimized Operation Strategies of Solar Thermal Power Plants. Selected Topics in Applied Earth Observations and Remote Sensing. Journal of Institute of Electrical and Electronics Engineers 2008;1(1):18-27.
[10] Wittmann M, Eck M, Pitz-Paal R, Müller-Steinhagen H. Methodology for Optimized Operation Strategies of Solar Thermal Power Plants with Integrated Heat Storage. Proc. SolarPACES 2009, Berlin, Germany; 2009.
[11] Powell KM, Hedengren JD, Edgar TF. Dynamic Optimization of a Solar Thermal Energy Storage System over a 24 Hour Period using Weather Forecasts. Proc. American Control Conference, Washington, DC; 2013.
[12] Hirsch T, Eck M, Blanco M, Wagner MJ, Feldhoff JF. Standardization of CSP performance model projection - latest results from the guiSmo project. Proc. ASME 2011 5th International Conference on Energy Sustainability, Washington, DC; 2011.
[13] García-Barberena J, Garcia P, Sanchez M, Blanco MJ, Lasheras C, Padrós, A, Arraiza J. Analysis of the influence of operational strategies in plant performance using SimulCET, simulation software for parabolic trough power plants. Journal of Solar Energy 2012;86(1):53-63.
[14] Wagner PH. Thermodynamic simulation of solar thermal power stations with liquid salt as heat transfer fluid. Diploma thesis, Technical University of Munich; 2012; Available from: http://elib.dlr.de/83921/.
[15] Pawellek R, Löw T, Hirsch T. EbsSolar – A solar library for EBSILON®Professional. Proc. SolarPACES 2009, Berlin, Germany; 2009.
[16] Hirsch T, Janicka J, Löw T, Metzger C, Pawellek R. Annual simulations with the EBSILON Professional time series calculation module. Proc. SolarPACES 2010, Perpignan, France; 2010.
[17] Pawellek R, Pulyaev S, Hirsch T, Wittmann M, Seitz M. Transient simulation of a parabolic trough collector in EBSILON®PROFESSIONAL. Proc. SolarPACES 2012, Marrakesh, Morocco; 2012.
[18] Meyer L, Band D, Gathmann N, Holten W, Roth M, Schmitz K. Optimisation of the configuration of parabolic trough power plants in the range of 250 MW. Proc. SolarPACES 2010, Perpignan, France; 2010.
[19] Burkholder F, Kutscher C. Heat Loss Testing of Schott's 2008 PTR70 Parabolic Trough Receiver. 2009; Available from: http://www.nrel.gov/docs/fy09osti/45633.pdf.
[20] Relloso S, Delgado E. Experience with molten salt thermal storage in a commercial parabolic trough plant. Andasol-1 commissioning and operation. Proc. SolarPACES 2009, Berlin, Germany; 2009.
[21] Hirsch T, Schenk H. Dynamics of oil-based parabolic trough plants - a detailed transient simulatio model. Proc. SolarPACES 2010, Perpignan, France; 2010.
[22] Pulyaev S. Untersuchung der instationären Prozesse im Kraftwerksbetrieb und deren Berücksichtigung in der Simulation mit EBSILON®Professional. Diploma thesis, Technical University Darmstadt; 2011.
[23] NREL. MIDC/University of Nevada, Las Vegas (36.06 N, 115.08 W, 615 m, GMT-8); Available from: http://www.nrel.gov/midc/unlv/.
[24] Müller-Elvers C, Wittmann M, Schubert A-C, Übler M, Ralph E, Hillebrand S, Saur M. Design and Construction of Molten Salt Parabolic Trough HPS Project in Évora, Portugal. Proc. SolarPACES 2012, Marrakesh, Morocco; 2012.